UTRECHT UNIVERSITY

Institute for Marine and Atmospheric research Utrecht (IMAU)

DETECTION AND QUANTIFICATION OF NATURAL GAS LEAKS USING MOBILE MEASUREMENTS IN AMSTERDAM

PAULA MAYNOU

Supervisors

Guus Velders

Thomas Röckmann

Hossein Maazallahi

Master Thesis

Science and Business Management

July 2022

ACKNOWLEDGEMENTS

I am thankful to Guus Velders and Thomas Röckmann for welcoming me at IMAU and helping me carry out my project through their supervision and encouragement. I am grateful to Hossein Maazallahi for his continuous advice and support. I also want to show my appreciation to Daan Stroeken, who helped me greatly with the measurements.

INDEX OF CONTENTS

ABSTRACT

Fast mobile detection of gas leaks in urban natural gas networks results in speeding up leak detection and repair procedures, thus reducing methane (CH_4) emissions and safety in urban areas. In this study, we carried out mobile measurements in the city of Amsterdam using high-precision methane analyzers installed in a van. As a result, 44 potential gas leaks were identified, i.e., leak indications (LIs), out of which 31 were quantified. Similar to other studies, a few large leaks in Amsterdam were contributing to a large proportion of the estimated total emissions. Two of the quantified LIs contributed to 76% of total emissions and these two leaks were fixed by the local gas distributor after locations were shared with the utility. The detection probability of significant CH_4 enhancement (more than 10% above background) on single passages was, on average, about 70% for the smaller leaks and increased to 100% with bigger estimated size. Overall, 73 % of the confirmed leaks were already detected on the first pass by the measuring van. Our results indicate that mobile CH_4 surveys can be a useful method that could be implemented in the management of natural gas (NG) distribution systems for faster detection of leak locations compared to common methods, and for leak quantification and repair prioritization in order to mitigate CH_4 emissions. Further mobile measurements and improvements in the data analysis process of this method in collaboration with local gas distributors will improve detection and emission quantification of gas leaks in the natural gas network.

PLAIN LANGUAGE SUMMARY

Global warming is the rapid increase of global temperature on our planet in the past decades. This is due to increased concentrations of greenhouse gases in the atmosphere, mainly from human activities. It is believed that global warming will cause large effects on the entire climate system. Methane (CH_4) is the second most abundant greenhouse gas, after carbon dioxide, and accounts for over 20% of radiative forcing of the climate systems. CH_4 is the main component of the natural gas that is used to heat homes and water and it has 85 times the global warming potential of carbon dioxide over a 20-year time period. Moreover, CH_4 has an atmospheric lifetime of about a decade whereas CO_2 can stay in the atmosphere for centuries. Therefore, reducing methane emissions will slow down the pace of warming in the near term and bring us closer to meeting the goals of the Paris Agreement, a universal agreement that sets out a framework to limit global warming and deal with the impacts of global climate change.

It is a fact that the natural gas distribution networks are a source of methane emissions due to leaks in the pipelines, which sometimes are quite old. However, there has been limited focus on urban methane emissions and these have generally been underestimated. This project has used mobile measurements with a car to identify, locate, and quantify leaks in the gas distribution network in the city of Amsterdam. The results show that this method could be implemented by the gas companies in order to find and fix leaks fast especially the bigger ones, since it was found that 73% of the leaks were detected on the first drive by the car and that as few as two leaks accounted for 76% of the total estimated emissions.

1. INTRODUCTION

An increase in global temperature has occurred in the past decades, largely attributed to the build-up of greenhouse gases in the atmosphere (IPCC, 2021). The already observable effects and the potential large repercussions it might have on the entire climate system (IPCC, 2022) have led to extensive research and to regional, national and international political initiatives such as the Paris Agreement or the Heat Transition Vision in Amsterdam (City of Amsterdam, 2020) to try to combat it. Global average methane (CH_4) mixing ratios in the atmosphere are currently 2.5 times greater than preindustrial levels and keep rising as a result of the growing industrialization, urban development, deforestation and agricultural intensification (NOAA, 2022; Hendrick et al., 2016).

Approximately, 40% of the CH_4 in the atmosphere is emitted by natural sources such as wetlands, volcanoes, permafrost, oceans, wildfires and termites (IEA, 2021; Van Amstel, 2012). The remaining 60% comes from anthropogenic sources. The biggest source, which accounts for almost half of the anthropogenic emissions, is agriculture (especially livestock farming), and the second largest source is energy production and use. The latter accounts for up to one third of the global anthropogenic CH_4 emissions (IEA, 2021), and includes oil, gas and coal mining. Other anthropogenic sources are landfills, wastewater treatment and biomass burning which, collectively, constitute about 20% of the anthropogenic global budget (Global Methane Initiative, 2011).

CH_4 is the second most abundant greenhouse gas after carbon dioxide (CO_2) with annual emissions that range from 594 to 880 Tg according to bottom-up estimates and 550 to 594 Tg reported by top-down approximations (Saunois et al., 2020). It is also a precursor to tropospheric ozone production (Plant et al., 2019) and an additional source of water vapor in the stratosphere through oxidization, which has a further radiative impact (Myhre et al., 2013). CH_4 has a global warming potential 85 times more powerful than CO_2 in a time span of 20 years and has an atmospheric lifetime of about a decade (Prather et al., 2012). Consequently, CH_4 mitigation would have a bigger impact in slowing down the rate of global warming in the near future compared to CO_2.

That is why cutting CH_4 emissions is key in the response to climate change, especially in cities, industrial centers and areas of intensive agriculture, which are the major sources. CH_4 emission reductions do not only have significant benefits for public safety but are also more easily attainable than CO_2 both technologically and economically (Hopkins et al., 2016). However, top-down (derived from atmospheric measurements) and bottom-up (derived from inventories) values of the global budget differ significantly. Location and strength of CH_4 sources are poorly known and quantified (Lowry et al., 2001; Defratyka et al., 2021), which leads to uncertainties and discrepancies in emission inventories. A better understanding of CH_4 emissions at a local scale is important in order to achieve effective mitigation strategies (Maazallahi et al., 2020; Defratyka et al., 2021).

Contrary to CO_2, CH_4 is released in large part as fugitive emissions that occur in nearly every step of the natural gas supply chain including extraction, processing, storage, transportation and use (Hopkins et al., 2016). These large emissions, caused by accident or not, are of major concern. Unfortunately, not all emission sources are inventoried but several studies conclude that, given the volume of gas distributed and used in cities, losses in urban areas are a significant component of urban anthropogenic emissions that can have a national-level impact (Plant et al., 2019). According to Hopkins et al. (2016), in highly populated industrial and urban regions such as Los Angeles and

Salt Lake City, the energy and waste sectors are the main sources of CH_4 emissions, making up about 45% and 40% of urban emissions respectively. More specifically, urban mapping and road surveys have shown how gas leaks from natural pipelines are responsible for most fugitive emissions of CH_4. A study estimated that, overall, 20 to 36 % of losses from the United Stated natural gas (NG) supply chain are due to distribution and end use only and that is why some mitigation strategies include reducing gas leaks in the distribution system (Sargent et al., 2021).

Despite the previously mentioned advantages of CH_4 emission reduction, there are considerable barriers to overcome in order to implement urban methane emission mitigation (Saunois et al., 2020). Emissions are usually underestimated in inventories, there is a significant variability between different cities and, most importantly, current approaches are inefficient or non-existent (Hopkins et al., 2016). Studies of quantification of urban CH_4 emissions and frequency of leaks (Plant et al., 2019) have emphasized the need to develop and implement customized mitigation plans of action in cities globally, and to establish monitoring strategies to evaluate reductions and increase the chances of success. The contribution of CH_4 emissions from different sources vary in each city (Maazallahi et al., 2020; Fernandez et al., 2022).

In a study carried out in Boston, losses from the natural gas storage and distribution system were determined to be two to three times larger than inventory methodologies estimated (Mckain et al., 2015), and gas leaks were found to be the largest contribution to CH_4 emissions in the cities of Hamburg, Germany (50%-80%) (Maazallahi et al., 2020), Paris, France (63%) (Defratyka et al., 2021), Florence, Italy (85%) (Gioli et al., 2012), and Utrecht, Netherlands (~70%) (Maazallahi et al., 2020). Moreover, a study carried out in London, UK, between 2012 and 2014, also found CH_4 emissions to be underestimated by the inventory approach since the measured emissions were more than twice the inventory value (Helfter et al., 2016). Several studies conducted in eastern U.S. cities indicate that the densely populated ones have thousands of gas leaks: 5893 in Washington DC (Jackson et al., 2014), 3356 in Boston (Phillips et al., 2013) and 1050 in Manhattan (Gallagher et al., 2015). Moreover, surveys in Washington, DC have uncovered dangerous leaks that are considered to be an explosive hazard (Jackson et al., 2014).

Numerous studies on gas leaks as well as incidents have brought attention to the aging of natural gas infrastructures since it is the older pipelines, made of grey cast iron, asbestos cement and bare steel, that cause the most leaks (Phillips et al., 2013; Jackson et al., 2014; Hendrick et al., 2016). This is the main reason why these pipelines are being monitored more closely and replaced by safer materials in cities such as Amsterdam. However, newer pipelines made of plastic and coated steel have also shown problems and aging effects similar to those made of iron (Weller et al., 2020).

According to the RIVM (National Institute for Public Health and the Environment) national inventory report, total CH_4 emissions in the Netherlands have decreased by 46% since 1990; mostly due to decreased emissions in the waste sector while emissions from the energy sector have not changed significantly (Wever et al., 2022). NG heats roughly 90% of homes and businesses in the Netherlands (City of Amsterdam, 2020). A study from 1995 analyzed CH_4 emissions in Amsterdam and focused on NG leaks as they were considered the main source of emissions from the NG transport and delivery system (Veenhuysen & Hofschreuder, 1995). However, emissions in the city might have significantly changed since then and not much more research has been carried out, let alone street-level mobile measurements. The 2019 (most recent) officially registered CH_4 emissions indicate that 11% of the 2400 tons emitted by Amsterdam are due to the distribution of NG

(Emission Registration, 2022). Moreover, gas distribution is classified as the main source of CH_4 (65%) within the energy sector in the municipality. Thorough understanding of pipeline leaks and accurate identification and risk assessment is crucial for repair and replacement strategies because main pipeline replacement can cost up to millions of dollars per kilometer (Forman, 2014). In Amsterdam, the average cost of repairing a distribution main (30 and 100 mbar) is 1802€ and 5250€ for a transport main (>200 mbar and up to 8 bar) (R. van Eekelen, personal communication, July 11, 2022).

Apart from natural gas leaks, there are other sources of CH_4 in urban areas such as sewage systems, vehicles or heating systems and also the canals, especially in the case of Dutch cities. These sources can be distinguished by measuring more compounds such as ethane (C_2H_6) and CO_2. In the case of natural gas, although CH_4 is the main component, it also contains other carbohydrates such as C_2H_6 or propane to a lesser extent. Moreover, in the case of vehicle combustion, CH_4 is accompanied by a high mixing ratio of CO_2. One of the aims of this study is to perform mobile CH_4 measurements in a representative area of Amsterdam in order to detect and quantify CH_4 emissions as well as attribute them to NG leaks.

This study extends the one carried out in Utrecht and Hamburg (Maazallahi et al., 2020) to Amsterdam in order to make a thorough analysis of the existing NG leaks in the capital of the Netherlands. Similar studies in cities in the U.S. found leaks that the local gas distribution companies were unable to locate with their equipment and expressed concern because some of the leaks discovered were categorized as grade 1 i.e., constituting a hazard and requiring immediate repair (Weller et al., 2018). Therefore, it is also a goal of this project to contribute to the current knowledge as well as to promote and lead further investigation and mitigation strategies not only in Amsterdam but in other major cities in the country.

1.1. Objectives

The objectives of this project are listed below and the main ones are those written in bold type.

i. Do bibliographic research on mobile measurements, CH_4 emissions and national inventories. Also, understand local sources of CH_4.

ii. Carry out measurement surveys in residential areas of Amsterdam to detect and locate natural gas leaks.

iii. Quantify the CH_4 emissions from gas leaks.

iv. Upscale emission estimates to the whole city of Amsterdam.

v. Compare the results to national inventory reports and studies from other cities.

vi. Discuss strengths and weaknesses of the quantification method.

vii. Assess the effectiveness of the technique for detecting gas leaks.

viii. Assist in reducing CH_4 emissions from the NG distribution network in Amsterdam.

2. MATERIALS AND METHODS

In this section, the measurement setup, instrumentation used, areas of Amsterdam that were mapped and driving strategy are described. The algorithm used for data preparation and analysis is explained as well as the methods for attribution and quantification of emissions. All these steps are illustrated in the flow diagram in section *2.7*.

2.1. Instrumentation

Mobile measurements were performed with a Volkswagen Transporter where two Picarro cavity ring-down spectroscopy (CRDS) gas concentration analyzers were installed on the backseat (see Supplementary Information S.1). The G2301 instrument provides atmospheric mole fraction values of CO_2, CH_4 and H_2O at about 0.3 Hz measurement rate with a reproducibility of 1 ppb for CH_4. Observed peaks are smoothed out because the measurement cell is flushed approximately every 3 seconds given its volume and pressure (*Figure 1*). The G4302 Gas Scouter, provided by TNO (Netherlands Organization for Applied Scientific Research), is a portable, battery-powered analyzer that provides atmospheric mole fraction data of CH_4, C_2H_6 and H_20 at 1 Hz sampling frequency. The instrument can be operated in C_2H_6/CH_4 mode and in CH_4-only mode. The C_2H_6/CH_4 mode, with a reproducibility of 15 ppb for C_2H_6 and 100 ppb for CH_4, was used for surveying in order to measure the ethane–to–methane ratio and determine the emission source. Mixing is insignificant compared to the G2301 because the cell is flushed in 0.01 seconds and, therefore, the peak in *Figure 1* is sharper.

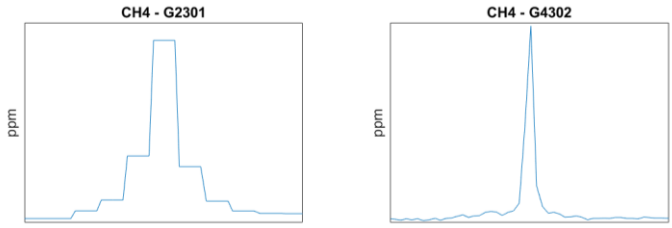

Figure 1: Example of the same CH_4 peak measured in ppm throughout a time period of 30 seconds (horizontal axis) with the G2301 (left) and the G4302 (right) analyzers. The G2301 peak is smoothed out because CH_4 readings are taken every 3 seconds whereas the G4302 peaks are sharper because the measurement cell is flushed much quicker.

The instruments sampled air from an inlet located at the front bumper of the van using a pump and teflon tubing (0.25 in). The tracks, locations and speed information from the surveys were registered with a GPS (Samsung device with GPS Logger app). The time shifts between the Coordinated Universal Time (UTC) and the Picarro instruments were corrected every day for each instrument. The time delay between air at the inlet and signal in the gas analyzers, which is caused by the length of the inlet tube, was also determined and accounted for when processing the data. This temporal offset was measured by exhaling in small CH_4 pulses into the inlet. The results of the different attempts, with a difference of 0.5 to 2 seconds between each other, were averaged each day for each instrument. Overall, the G2301 was used for both quantification and attribution whereas the G4302 was used mainly for attribution. However, the latter was convenient for measuring on foot, getting closer to the sources and pinpointing the exact location of leak indications (LIs).

2.2. Target city: Amsterdam

Amsterdam is the capital of the Netherlands with a population of 0.9 million and a density of over 5,200 inhabitants per km^2. It is the largest city in the country and a good candidate for this study given that no surveys of this kind have been carried out in Amsterdam while other cities such as Utrecht (Maazallahi et al., 2020); Paris (Defratyka et al., 2021), Boston (von Fischer et al., 2017) or Toronto (Ars et al., 2020) have already been mapped. Furthermore, some of the old pipelines in the Dutch capital are made of grey cast iron and asbestos cement, which are more leak prone materials and are set to be completely replaced by newer ones in the next ten years due to new regulations. The big cities in the Netherlands are very densely populated and, according to CBS (Statistics Netherlands), approximately 92% of households were using natural gas for heating in 2019 (CBS, 2021). It has been estimated that 65% of emissions from electricity generation and NG and oil production and distribution in the Netherlands are due to leaks in the distribution network, which at the same time account for 11% of total CH_4 emissions in the municipality of Amsterdam (Emission Registration, 2022).

The whole city was not mapped completely in this study. Instead, several areas were surveyed to then extrapolate the results to the whole of Amsterdam. To identify the neighborhoods of interest we focused on residential areas and used a map of the grey cast iron and asbestos cement pipelines published on the website of the gas company Liander showing their pipeline replacement progress (Liander, 2022). However, the age of the pipelines was not considered because this information was not made available by the company. The areas that were covered in this study are shown in *Figure 2* and mainly constitute the East and Old South of the city: Watergraafsmeer, Zeeburg, Dapperbuurt, Oosterparkbuurt, Weesperbuurt en Plantage, Oud-Zuid, De Pijp and Rivierenbuurt. Oud-West and the center (Jordaan and Grachtengordel) were also areas of interest but were not surveyed due to limited availability of the van and also because quantification of LIs and a thorough evaluation of the method were prioritized instead of covering a larger area of the city, which would only have been possible to sample once. Moreover, some leaks found in the Port of Amsterdam while doing measurements for a different project are also included in the results of this study.

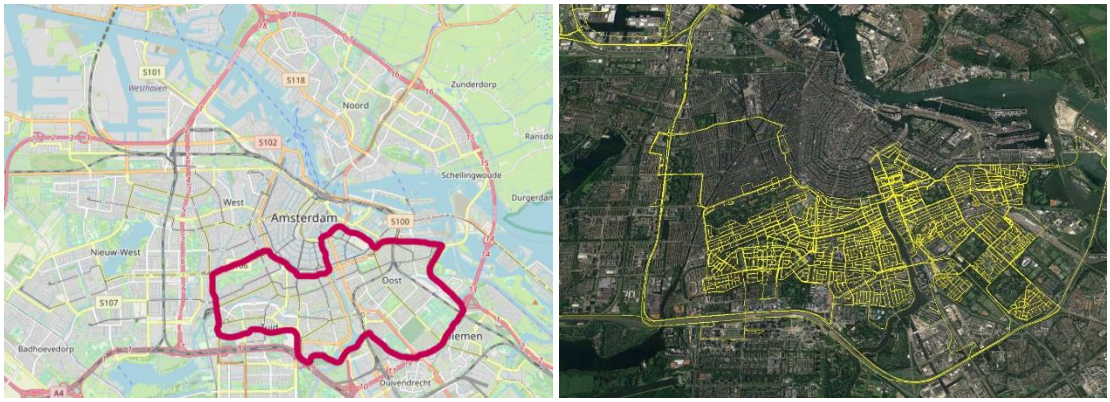

Figure 2: Study area in Amsterdam (left) and tracks of measurement routes (right).

2.3. Measurements and driving strategy

Surveys were usually carried out between 09:00 and 18:00 LT on days of minimal to no rain and with average driving speeds ranging from 10 to 20 km h^{-1}. The effect of rain on measurements was tested directly at 2 LI sources (see Supplementary Information SI.2). Rainwater blocks the pores and small cracks in the ground through which the CH_4 comes out. Approximately, the CH_4 mixing ratio values decreased to 5 – 20% compared to a dry day and C_2H_6 mixing ratios were reduced to 15 – 25%. Generally, the driving strategy was to cover all streets of the designated study area and afterwards revisit the locations where a CH_4 elevated reading or clear peak was observed. As explained in Weller et al. (2019), an elevated reading is defined as having CH_4 enhancement levels greater than or equal to 10% of the background. However, narrow and localized peaks with lower signals were also revisited in this study in an effort to detect and quantify the smaller leaks.

As opposed to other studies in other cities that used Google Street Cars and covered all the streets at least twice (Weller et al., 2018), we had one van and a limited amount of time. So, at first, we drove through all the streets once and then did a second measurement only at locations with CH_4 enhancement. If a CH_4 enhancement was detected for a second time when revisiting, 6 to 12 transects were performed. Verification of observed LIs is important because not all enhancements are due to gas leaks but can also be biogenic or from vehicles. Transects are also necessary for both attribution purposes and quantification of gas leaks. Numerous factors such as weather, wind, soil conditions, surface type, traffic, urban geography and distance between the survey car and the leak indication can affect the measured plumes. A previous study (Luetschwager et al., 2021) highlights the importance of obtaining multiple observations of the same source over different hours and days as well as the need for a minimum of 6 to 8 transects. According to Luetschwager et al. (2021), greater sampling effort reduces variation in size estimates to around 10% and increases gas leak detection probability to over 90%.

Overall, 2,700 km were driven over the course of 23 days of measurements (see Supplementary Information SI.3). Approximately, 330 km of roads were covered in Amsterdam, where 155 locations with enhancement were recorded, 75 of which were revisited at least once. In a few cases, leaks could not be quantified because, when revisiting LIs for the second or third time, they had disappeared and we suspect that they had been fixed in the meantime. Having two monitoring screens with real time data of the measurements from the two Picarro instruments was very useful while performing the measurements, for confirming and discarding LIs in situ, as well as for performing transects. Moreover, when measuring on foot with the G4302, the real time data made it possible to find the exact locations of the leaks.

2.4. Data preparation

The first step in the evaluation is the extraction of the useful data from each instrument and selection of the time period of actual measurements. Next is the application of the time correction explained in section *2.1* and the calibration functions (Maazallahi et al., 2020). This is followed by synchronization of the data from both instruments with the GPS.

Leak detection is based on identification of elevated CH_4 concentration readings. These departures from typical concentration levels of CH_4 are characterized by previously defining a background or baseline. Atmospheric mixing ratios are typically around 2 parts-per-million (ppm) but background levels are highly variable within cities and in time, so a background has to be defined as a function of local measurements (von Fischer et al., 2019). This is calculated using the lower 5th percentile of the concentrations recorded within ±2.5 minutes of measurements for each individual point (Maazallahi et al., 2020; Weller et al., 2019). The background is then subtracted from the measured mixing ratios in order to obtain the enhancement for both CH_4 and CO_2. For C_2H_6, the background is calculated in the same way and set to zero as its mole fraction is usually around 0.4 – 2.5 ppb, which is lower than the G4302 detection limit. Moreover, to eliminate noise from the G4302, all data values below 0.01 ppm are set to zero. Google Earth files are generated from CH_4 enhancement (*Figure 3*).

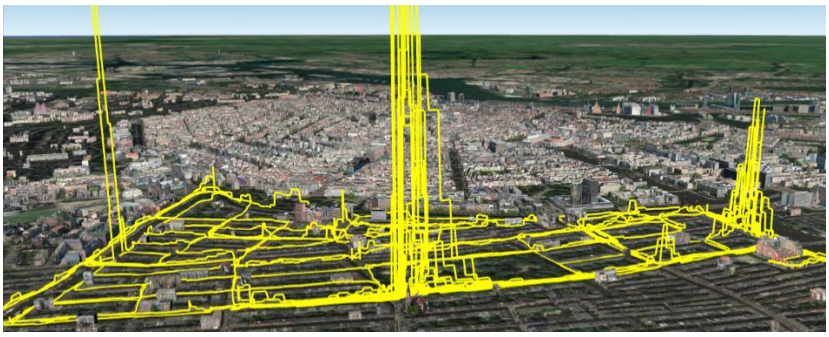

Figure 3: Google Earth image of CH_4 concentration enhancements from mobile measurements in De Pijp, Amsterdam.

2.5. Emission attribution

As previously mentioned, both CH_4 and C_2H_6 are components of NG. Therefore, analyzing the correlation and ratio between these two compounds is an effective method for determining whether the source of measured CH_4 is NG or not. Other sources of CH_4 can be swamp gas, sewer systems, compressed natural gas vehicles (Curran et al., 2014), incomplete combustion (Nam et al., 2004) or canals.

The criteria for attributing an observed CH_4 concentration peak to NG was a minimum enhancement on the G4302 of 0.5 ppm for CH_4 and 15 ppb for C_2H_6, and a linear regression coefficient of at least 0.7 between the two compounds (Maazallahi et al., 2022). In the Amsterdam surveys, the point-to-point C_2H_6: CH_4 ratio was 3.6 ± 0.6 %, which is very similar to the 3.9 ± 0.8 % ratio obtained in Utrecht (Maazallahi et al., 2020). Therefore, locations with higher ratios or R^2 lower than 0.7 were not considered leaks. Moreover, the CH_4: CO_2 ratio can also be used for attribution since combustion

processes emit both CH_4 and CO_2. As in Maazallahi et al. (2020), locations with CH_4: CO_2 ratios of 0.02 – 20% and R^2 higher than 0.8 were attributed to combustion.

2.6. Emission quantification

Quantification of leak emission rates is made using the equation given in Weller et al. (2019). Using the same approach allows comparable results between different cities both in Europe and the US. This empirical equation (Eq 1) is based on a set of controlled release experiments in different environments with Picarro G2301. Moreover, it assumes an average distance of approximately 16 meters between the car and the leak.

$$\overline{ln(CH_4\ enhancement)} = -0.988 + 0.817 \cdot ln\ (emission\ rate) \qquad \textbf{Equation 1}$$

Equation 1: Equation used to convert CH_4 enhancements from gas leaks measured with a Picarro G2301 in a moving vehicle into emission rates. CH_4 enhancements are in parts per million (ppm) and emission rates are in liters per minute (L min^{-1}).

The emission rate of a LI is obtained by taking the natural logarithm (*ln*) of the maximum enhancement values of all observed peaks in the specific location and calculating the average. This value is then entered on the left side of *Equation 1* and it is solved for the emission rate. The calculated estimates are categorized into three classes, as in von Fischer et al. (2017): high (>40 L min^{-1}), medium (6–40 L min^{-1}) and low (0.5–6 L min^{-1}).

CH_4 enhancement values can vary between different observations both minutes or days apart and this can produce large uncertainties for quantification of individual LIs. An analysis of the variation in leak size estimation is done in Luetschwager et al. (2021) and the relationship between the number of detections and variation in size estimates is discussed. It is concluded that after six detections the average difference declines to approximately 10%. Consequently, in this study, a minimum of 6 detections and an average of 15 are used in the quantification process for each LI individually.

Finally, the emission rates of all detected leaks are summed to estimate the total emissions from the NG distribution network in the surveyed areas and these results are also scaled up using the total road length of Amsterdam compared to the road covered in the target study area.

2.7. Flow diagram

In *Figure 4,* the attribution step aims to illustrate how some LIs were not discarded right away after the first drive due to lack of C_2H_6:CH_4 correlation but some were instead revisited in order to increase the probability of detection and assess the method. In the case of confirmed leaks, revisits were made to obtain more data for quantification.

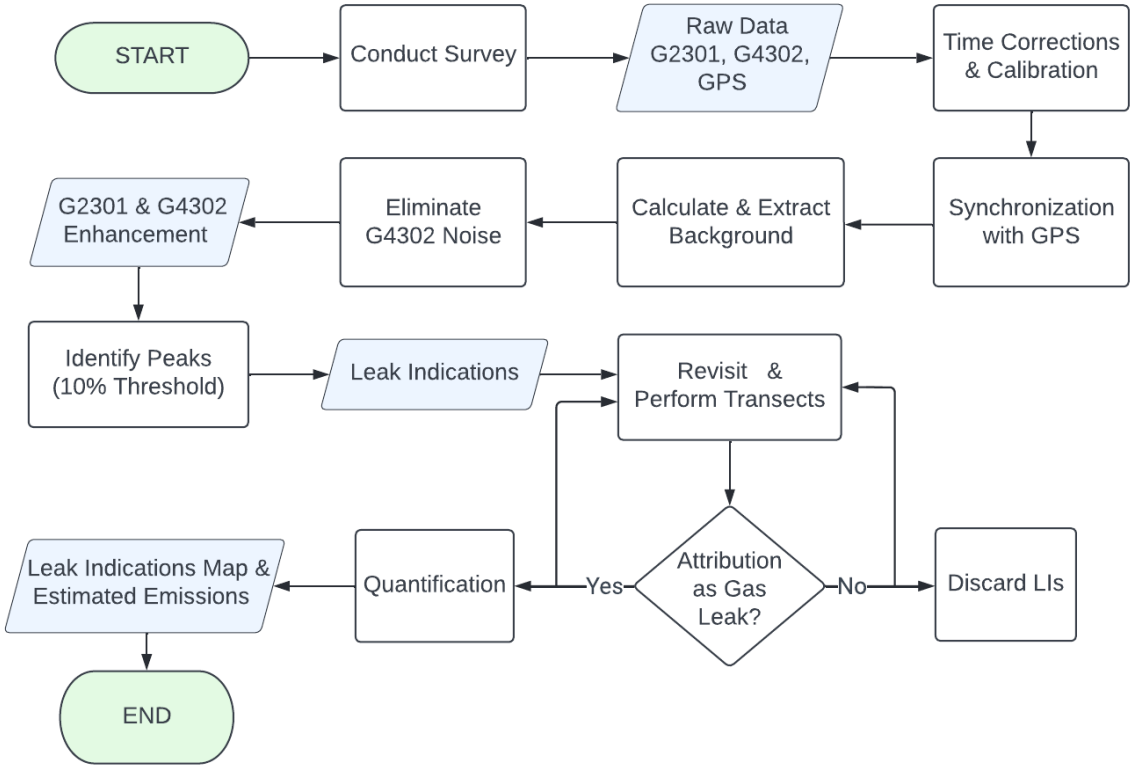

Figure 4: Flow diagram of the evaluation process of all leak indications including data preparation, attribution and quantification.

3. RESULTS AND DISCUSSION

Examples of attribution are discussed here along with an overview of all LIs and their estimated emission rates. The results are then extrapolated to the whole city and compared to both the studies in Utrecht and Hamburg, and the registered emissions for the municipality of Amsterdam (Emission Registration, 2022). Moreover, this section assesses the method employed by discussing instrument dependency of the quantification process, temporal variability of the measured plumes and leak detection probability. Strengths and weaknesses are considered and the impact of this project is evaluated in terms of reduced emissions. See pictures of measured locations in Supplementary Information SI.6.

3.1. Attribution

A total of 44 fossil CH_4 locations were detected, 59% of the revisited LIs. Overall, 33 of these LIs were confirmed and attributed to NG leaks from the distribution network based on a minimum of two observations of CH_4 enhancement above the 10% threshold and a clear C_2H_6:CH_4 correlation. In some occasions the ethane-mode of the instrument was faulty so attribution through correlation was not useful and some locations had to be evaluated individually and/or revisited. *Figure 5* is an example of a transect at a confirmed gas leak. Therefore, it shows C_2H_6:CH_4 correlation with a point-to-point ratio of 3% but no CH_4:CO_2 correlation. On the contrary, *Figure 6* shows an example of combustion, hence the large CO_2 mole fraction and opposite correlations. Overall, the confirmed and quantified leaks, with at least 10 transects, have an average C_2H_6:CH_4 ratio of 3.5 ± 0.6 % and a C_2H_6:CH_4 correlation probability of 60%. Furthermore, 71% of the LIs detected and attributed to fossil CH_4 on the first drive were later verified as gas leaks.

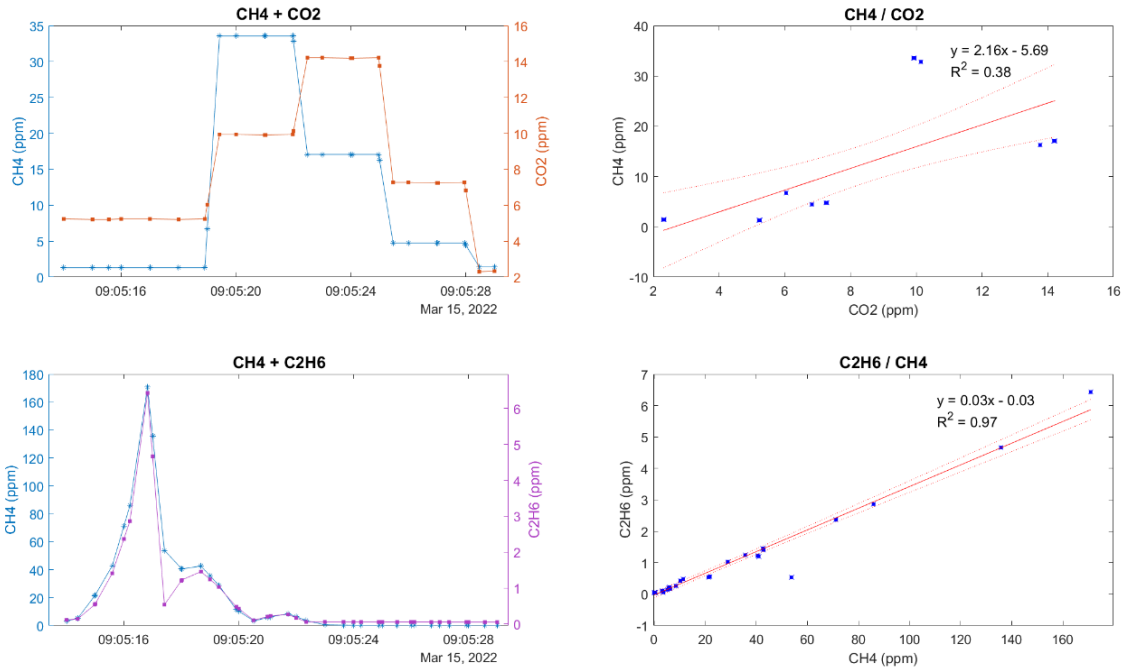

Figure 5: Example of using non CH_4:CO_2 correlation (above) and C_2H_6:CH_4 correlation (below) for attribution of CH_4 signal to gas leak. Left: enhancement concentrations over time; right: correlation between compounds, linear regression equation and correlation coefficient. The G2301 peaks (above) are smoothed out because CH_4 and CO_2 readings are taken every 3 seconds whereas the G4302 peaks (below) are sharper because the measurement cell is flushed much quicker.

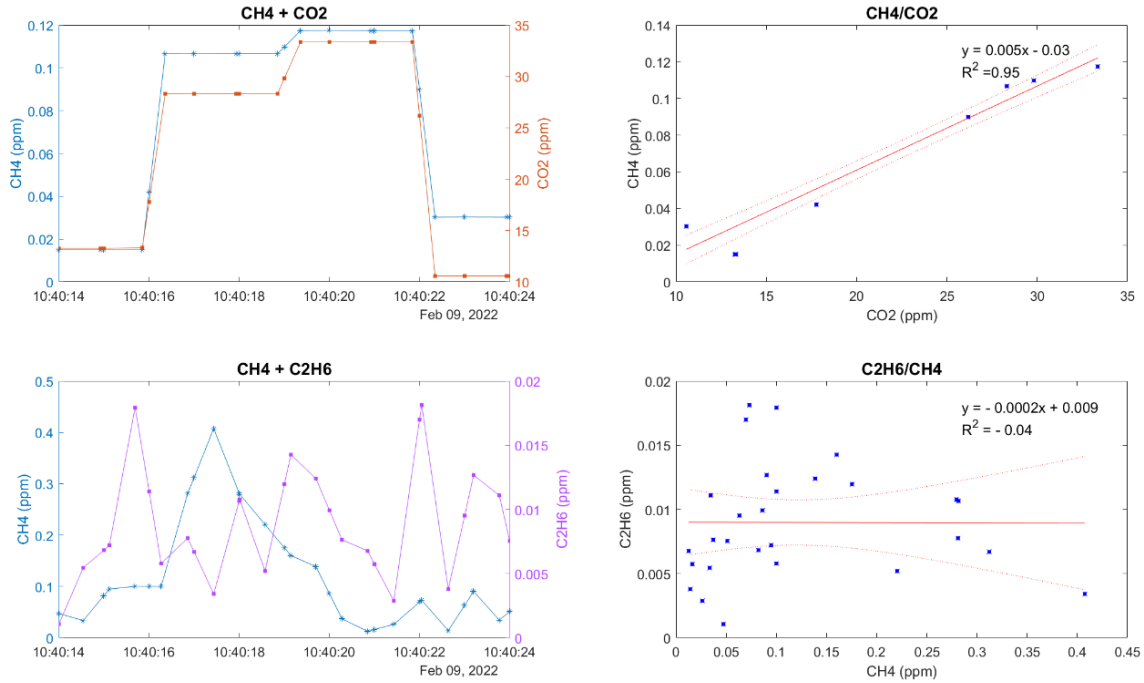

Figure 6: Example of using CH_4:CO_2 correlation (above) and non C_2H_6:CH_4 correlation (below) for attribution of CH_4 signal to gas leak. Left: enhancement concentrations over time; right: correlation between compounds, linear regression equation and correlation coefficient. The G2301 peaks (above) are smoothed out because CH_4 and CO_2 readings are taken every 3 seconds whereas the G4302 peaks (below) are sharper because the measurement cell is flushed much quicker.

Those locations where a CH_4 peak was observed several times but no C_2H_6 or CO_2 enhancement was detected were classified as microbial sources. An additional attribution technique such as isotopic analysis of $\delta^{13}C$ and δD, as in Maazallahi et al. (2020) and Fernandez et al. (2022), could complement the results from this section.

3.2. Emission quantification

As mentioned, 33 fossil CH_4 locations were confirmed as gas leaks and put into the high confidence LIs category and the other 11 remain unclassified and were therefore put in the low confidence LIs group (see Supplementary Information SI.4 & SI.5). As mentioned, high confidence entails that the LIs were observed at least twice with both CH_4 enhancement above the 10% threshold and a clear C_2H_6:CH_4 correlation. On the other hand, unclassified LIs either had enhancement below the 10% threshold or C_2H_6 was only observed once. Therefore, these LIs could also simply be end-use CH_4 peaks from houses. Furthermore, not all LIs in both groups could be quantified due to lack of data from a valid transect, i.e. CH_4 enhancement (see *Table 1*).

Table 1: Overview of all LIs in Amsterdam study area.

All locations	155
Revisited locations	75
Fossil CH_4 locations	44
High confidence LIs	33
Quantified	31
Low confidence LIs	11
Quantified	8

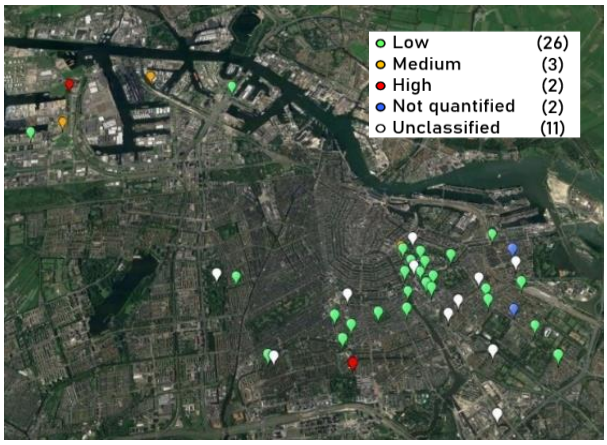

Figure 7: Categorized locations of significant LIs in Amsterdam study area.

As shown in *Table 2* and *Figure 8*, the confirmed leaks found in both the study area (26) and the Port of Amsterdam (5) were quantified with *Eq 1* and categorized into three classes: low (0.5 – 6 L min^{-1}), medium (6 – 40 L min^{-1}) and high (>40 L min^{-1}) emission rate, as in von Fischer et al. (2017). Overall, 510 transects were performed at locations of confirmed leaks, but only the transects with a CH_4 enhancement of about 0.2 ppm or higher were used for quantification, which were 73% of the total.

Table 2: Quantification and categorization of confirmed leaks and total emissions in surveyed area in Amsterdam.

Quantified LIs and emissions		Total number of LIs	31
		Total emission rate	297 L min^{-1}
LIs categorized	High >40 L min^{-1}	Number	2
		Emissions	225 L min^{-1}
		Average emission rate per LI	112.5 L min^{-1} per LI
		Percent of total emissions	76%
	Medium 6 – 40 L min^{-1}	Number	3
		Emissions	23 L min^{-1}
		Average emission rate per LI	7.7 L min^{-1} per LI
		Percent of total emissions	8%
	Low 0.5 – 6 L min^{-1}	Number	26
		Emissions	49 L min^{-1}
		Average emission rate per LI	1.9 L min^{-1} per LI
		Percent of total emissions	16%

The cumulative emission curve in *Figure 9* is constructed by first ranking the leaks from largest to smallest based on their estimated emission rate and then calculating the proportion of estimated total emissions. It indicates that the top 4 leaks (13% of leaks) account for approximately 80% of the total measured emissions. This is in line with the results from other NG leak studies that also found a small proportion of leaks to be responsible for the majority of emissions (Weller et al., 2018; von Fischer et al., 2017). Consequently, the low-rate leaks, which are far more common (84%), only contribute to 16% of the total emissions.

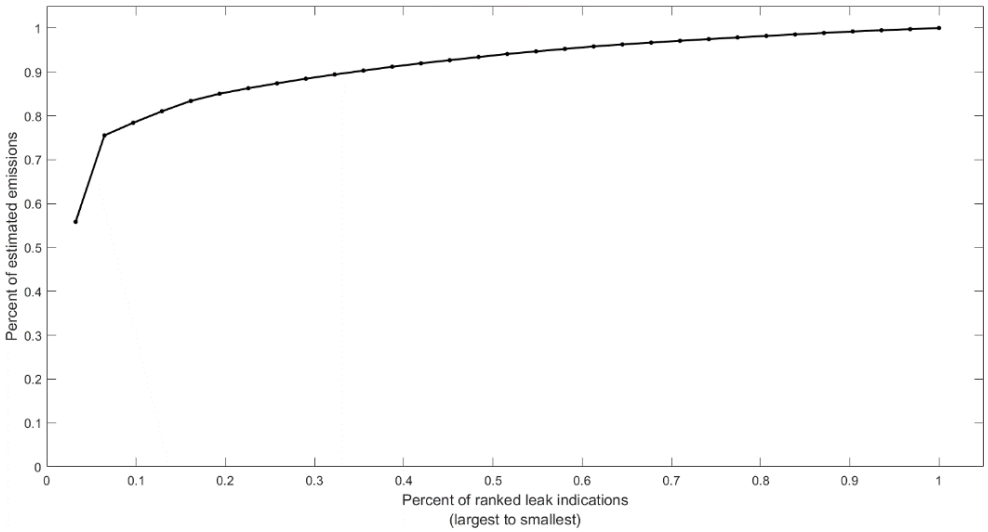

Figure 8: Cumulative CH_4 emissions curve from the mobile quantification method. The high and medium-rate leaks are less common (16%) but contribute to 84% of the total calculated emissions.

Something that this quantification technique fails to take into account is the distance between the car and the LI, which is different for each leak or even transect but is an important factor in the relationship between the emission rate and the excess CH_4 mixing ratios. However, it is difficult to estimate the exact distance because, initially, the location of the leak is unknown. *Equation 1* assumes an average distance of 16 meters (Weller et al., 2019) but further studies could adapt it to have a distance input so as to not underestimate the size of leaks at 15-20 meters or overestimate those at 0-5 meters, as discussed in von Fischer et al. (2017).

3.3. Extrapolation

The estimated emissions from 26 leaks in the study area were extrapolated to the whole urban area of Amsterdam, as shown in *Figure 9* In order to scale up the results, the total road length within the designated area is calculated with ArcGIS and it is assumed to be equivalent to the length of pipeline. Particularly, only the primary, secondary, tertiary, residential and unclassified roads from the Open Street Map Amsterdam file are included, which are the drivable streets in residential areas, not highways (Open Street Map, 2022). Overall, the study area makes up 22% of the total road length used to extrapolate. Contributions from the 5 leaks found in the Port of Amsterdam are left out for the extrapolation since this area was not originally included in this study because it is not residential. *Table 3* summarizes these calculations and compares them to the results obtained in Utrecht and Hamburg. The approach is different in this study since it focuses solely on emissions from gas leaks whereas the studies in Utrecht and Hamburg quantified all CH_4 enhancements and later estimated the proportion of LIs that correspond to NG leaks from the distribution network. Moreover, Hamburg's LI area density is considerably lower, which is probably because the area of extrapolation includes

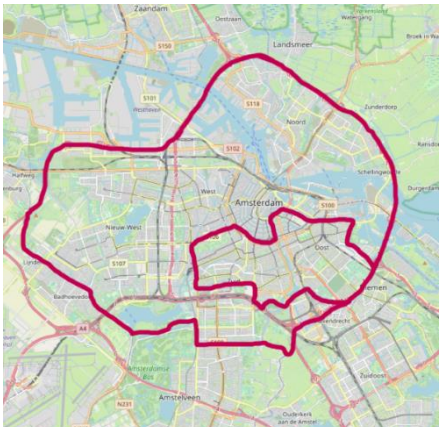

Figure 9: Map of Amsterdam study area and extrapolation area.

large green areas as well as the airport. In the case of Amsterdam, the airport is not within the boundary of extrapolation. Therefore, the LI densities per square kilometer of these three cities is are not really comparable. For the most part, the results are relatively similar for all three cities taking into account their different sizes.

Table 3: Summary of extrapolated emissions and comparison to Utrecht and Hamburg results (Maazallahi et al., 2020).

	Amsterdam	**Utrecht**	**Hamburg**
Kilometers covered	330 km	450 km	1200 km
Total number of LIs	44	81	145
Total emission rate (all LIs)	140 L min^{-1}	290 L min^{-1}	490 L min^{-1}
Total number of gas leaks	26	54	48
Gas leak density	12.7 km per leak	8.3 km per leak	24.8 km per leak
Total emission rate (gas leaks)	110 L min^{-1}	200 – 260 L min^{-1}	240 – 390 L min^{-1}
Average emission rate per leak	4.2 L min^{-1}	3.8 – 4.8 L min^{-1}	5.1 – 8.1 L min^{-1}
Emission factor	0.33 L min^{-1} km^{-1}	0.47 ± 0.14 L min^{-1} km^{-1}	0.19 ± 0.03 L min^{-1} km^{-1}
Kilometers of road	1500 km	650 km	3000 km
Upscaled LI emissions	640 L min^{-1}	420 ± 120 L min^{-1}	1200 ± 170 L min^{-1}
Upscaled gas leak emissions	500 ± 120 L min^{-1}	290 – 380 L min^{-1}	600 – 960 L min^{-1}
Area covered	18 km^2	45 km^2	396 km^2
LI density	0.7 km^2 per LI	0.6 km^2 per LI	2.7 km^2 per LI

In general, the emission factors from the NG distribution network found in European cities are lower than those in the US. Defrtyka et al. (2021) reported 0.16 L min^{-1} km^{-1} in Paris whereas von Fischer et al. (2017) obtained 2.3 L min^{-1} km^{-1} in both Boston and Staten Island, and 1.3 L min^{-1} km^{-1} in Syracuse. Total emission estimates range from 100 to 400 tons per year in Amsterdam, Utrecht, Hamburg and Paris while estimates go up to 1300 tons in the already mentioned US cities (von Fischer et al., 2017).

3.4. Comparison to national inventory reports

In order to compare the results of the surveys to the registered emissions in Amsterdam from 2019, emissions from the study area were extrapolated to the whole municipality which, in addition to the previously defined urban area (*Figure 9)*, also includes the port of Amsterdam, Zuid Oost and a large green area in the north.

The emissions registration reports a total of 267 tons of CH_4 emitted in 2019 only from gas distribution (Emission Registration, 2022). Similarly, our extrapolation results in emissions of 247 t CH_4 $year^{-1}$. However, if the study area is extended to include the port and, therefore one of the two high-rate leaks, yearly emissions increase up to 514 t, which doubles the initially estimated emissions.

The latter value might not be representative yet it effectively shows how one quick survey with these mobile measurements can detect a sporadic big leak and get it fixed before it can have a significant impact in the total annual emissions. In conclusion, the calculated estimates range from 247 to 514 tons per year whereas the inventory values have ranged between 267 and 286 tons throughout the 8 reported annual emissions in the past 32 years.

3.5. Instrument dependency

Equation 1 was defined specifically for CH_4 measurements from the Picarro G2301 and cannot be applied to maximum enhancement values from the G4302 for leak quantification since mixing ratios from G4302 are significantly higher (see *Figure 11* and Supplementary Information SI.7). Total estimated emissions are 297 L min-1 when calculated with the G2301 and 2052 L min^{-1} when calculated with the G4302. However, if the areas below the peaks (calculated with enhancement above background and distance) are used instead of the maximums, there is a strong correlation between the two instruments and their ratio is practically 1/1. For both graphs in *Figure 11*, the y-intercepts were forced to zero.

The earlier mobile quantification approach described in von Fischer et al. (2017) used both the plume height and area but the updated version by Weller et al. (2019) relies solely on plume height. Thus, this equation could be revised and improved, and controlled experiments could be performed in order to include a plume area input.

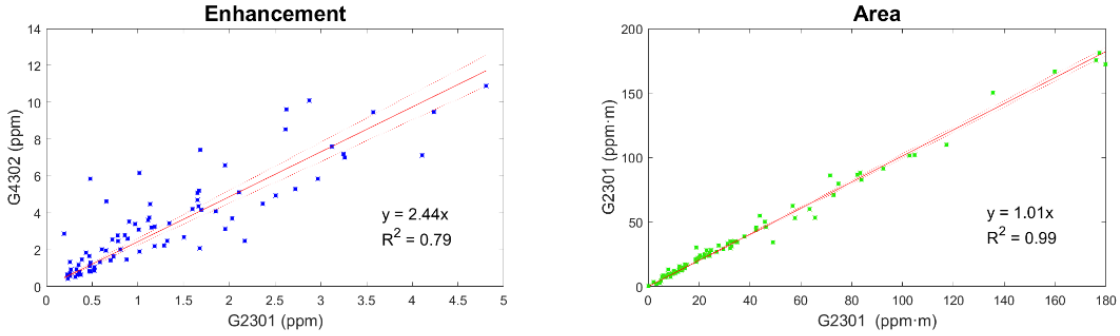

Figure 10: Correlation plots between the G2301 and G4302 for CH_4 concentration enhancement (left) and plume area (right). This comparison shows that, while the enhancement values differ between instruments, values of CH_4 plume areas are the same for both.

3.6. Temporal variability

In this section, ENVI-met, a microclimate CFD (Computational Fluid Dynamics) model for urban environments (ENVI-met GmbH, 2022), is used to discuss temporal variability when measuring LIs. This qualitative gas leak simulation at a street intersection (*Figure 11*) illustrates the previously discussed variability of measured plumes due to frequent changes in wind direction. If the car is driven from right to left all four times and only a few minutes apart, the observed enhancement is different for each transect. Therefore, the location has to be sampled more than once in order to get an accurate estimate of the emission rate.

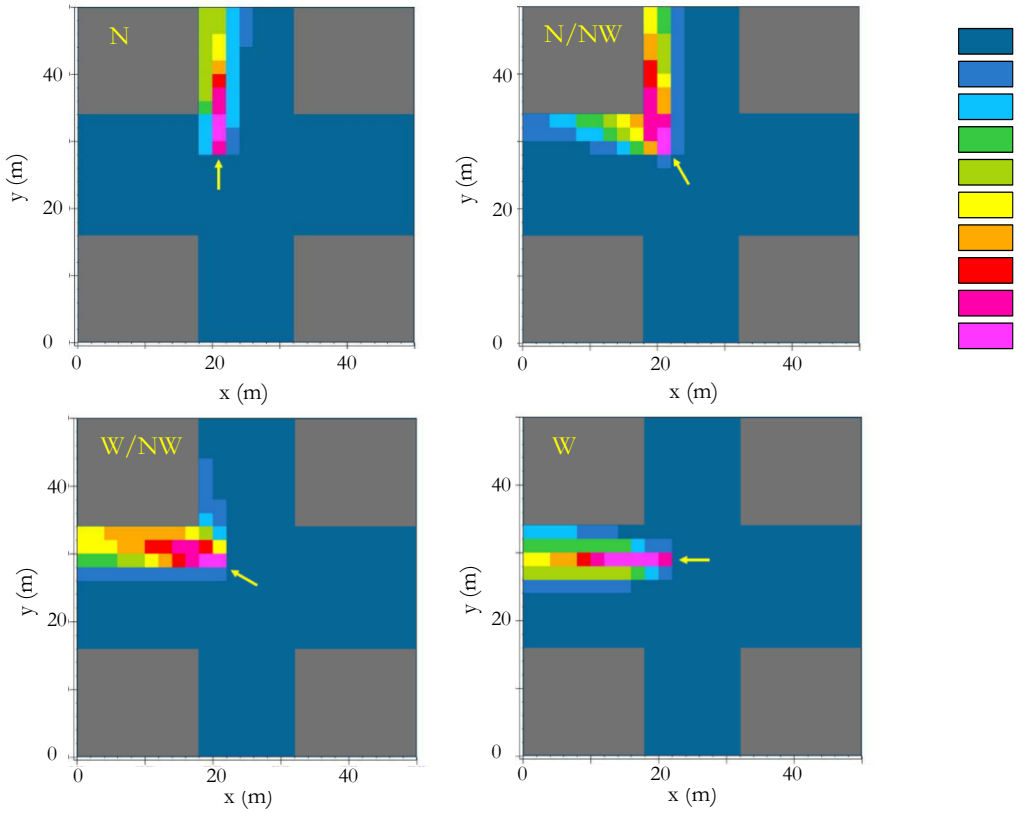

Figure 11: Gas leak plume simulation with different wind directions (yellow arrow). The grey boxes represent buildings and it is assumed that the vehicle is driven from right to left in all four cases. The color scale on the right shows the CH_4 concentrations (µg m^{-3}) in the plume from highest (pink) to lowest (blue). Simulation made with ENVI-met.

Figure 12 displays individual transect enhancement values measured on two or three different days for six confirmed leaks. As expected, despite the large range of values, when sampling the plume several times, the daily average is consistent between days (See Supplementary Information SI.9 *Table 12*). Therefore, a minimum of 6 to 8 transects are needed for accurate emission rate estimation. About one third of the quantified leaks in the study area had less than 6 valid transects, half of them due to enhancement being too small for detection. Including the quantification of these leaks with fewer transects in the results does not have a significant impact on the total estimated emissions since they are small leaks with rates ranging from 0.7 to 2.2 L min^{-1}. However, this brings up the issue of small leak overestimation. It has been discussed in other studies how for the smaller leaks the majority of maximum enhancement values tend to fall under the 10% threshold and only the few higher outliers can be used for quantification, thus giving larger emission rates (von Fischer et al., 2017; Weller et al., 2018). Even though overestimation of one individual small leak is not significant to the total, 84% of the quantified leaks in this study are in this category and can therefore have an impact as a whole. It is partly for this reason that emission variability of small leaks tends to be lower, because only enhancement values of about 0.2 ppm or higher are used for quantification whereas for bigger leaks, there is a lower limit for CH_4 excess mixing ratio and all transects are valid for quantification, which also leads to less transects. However, as shown in the Supplementary Information SI.9 *Table 13*, the range of emission rate values relative to leak size tends to be bigger for medium sized leaks, possibly because the measured plumes from these leaks are more affected by weather, soil and traffic conditions than the largest leaks.

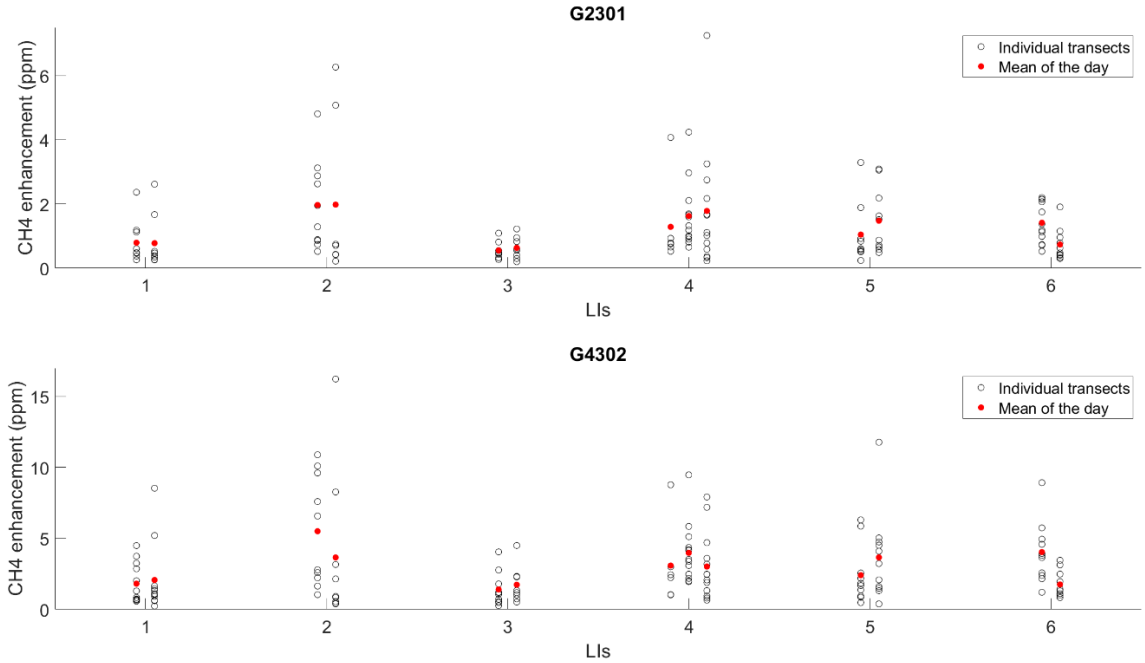

Figure 12: Temporal variability in CH_4 enhancement of 6 sampled gas leak locations. Shown are the enhancements of the individual transacts (open circles) and their daily average (red circles) measured with the G2301 and G4302 instruments.

3.7. Detection probability

The mobile measurement method that was employed in this study has proven to be highly effective for gas leak detection since 73% of leaks were already found on the first drive through excess CH_4 and C_2H_6 mixing ratios and a clear correlation between these two compounds. *Table 4* shows all detection results of the first drive in relation to the 33 high confidence LIs.

Table 4: Summary of leak detection on first survey drive. Number of leaks detected in first drive and percentage of first detections to the total number of leaks.

Detection of confirmed leaks (33)	1st drive	Percentage
CH_4 above 10% threshold	29	88%
C_2H_6 correlation	24	73%
C_2H_6 & CO_2 correlation	3	10%
CO_2 correlation	1	3%

Moreover, the 24 verified leaks are used in *Table 5* to assess detection probability, i.e. the likelihood that enhanced levels of CH_4 will be detected on a single transect of a gas leak. These leaks were quantified with at least 10 valid transects. They are also separated into high, medium and low categories to evaluate the relationship between detection probability and estimated leak size. Section SI.10 in the Supplementary Information shows detection probabilities as a function of estimated leak size (for medium and low emission rates). In general, for emission rates greater than 3 L min^{-1}, detection probabilities remain above 80%. In the case of CH_4 detection with the G4302, detection probabilities are higher, but not as high as for C_2H_6, where most probabilities exceed 80% already at 1 L min^{-1}. Given that correlation probabilities are the lowest and C_2H_6 detection probabilities are the highest regardless of leak size, maybe the detection criteria for C_2H_6 should be increased to a minimum enhancement of 20 ppb.

Table 5: Detection probabilities of G2301 and G4302 for a single drive-by.

	Detection probability of quantified LIs			
LI categories	**G2301 - CH_4**	**G4302 - CH_4**	**G4302 - C_2H_6**	**C_2H_6:CH_4 correlation**
High	100%	100%	98%	79%
Medium	96%	96%	97%	91%
Low	66%	71%	87%	53%

3.8. Reduced emissions

The two high-rate leaks (LIs 60 and 76 in SI.4), with joint emissions of 225 L min^{-1}, described in *Table 2* were immediately reported to the gas company in Amsterdam. The biggest one, in the port, was fixed within an hour, and the one in the study area, next to Beatrixpark, was fixed after a couple of days. In *Table 6*, a few comparisons and equivalences illustrate the impact of this project on CH_4 emissions in Amsterdam. The CO_2 equivalent emissions are calculated with a 20-year global warming potential of 84 and for the number of cars an average of 1800 kg of CO_2 $year^{-1}$ car^{-1} is assumed.

Table 6: Reduced emissions from this project assuming that the leak rates are constant over the whole year.

Number of fixed leaks	2
Total emission rate of fixed leaks	225 L min^{-1}
Percentage of total emissions	76 %
CO_2 equivalent emissions per year	7.1x10^6 kg CO_2 -eq $year^{-1}$
Number of cars equivalent	3942 cars $year^{-1}$
Cost of NG (for consumers)	153,000 € $year^{-1}$

Also, a third leak indication, LI 76 (SI.4), was reported to the gas company but was later dismissed as a gas leak because neither C_2H_6 nor THT (C_4H_8S, commonly added odorant) were measured by their team. However, we observed CH_4 and C_2H_6 enhancement at this location several times, as well as clear correlation (*Figure 13*), and even measured it up close (see Supplementary Information SI.8). So, we suspect that this could have been a measuring mistake on the part of the company.

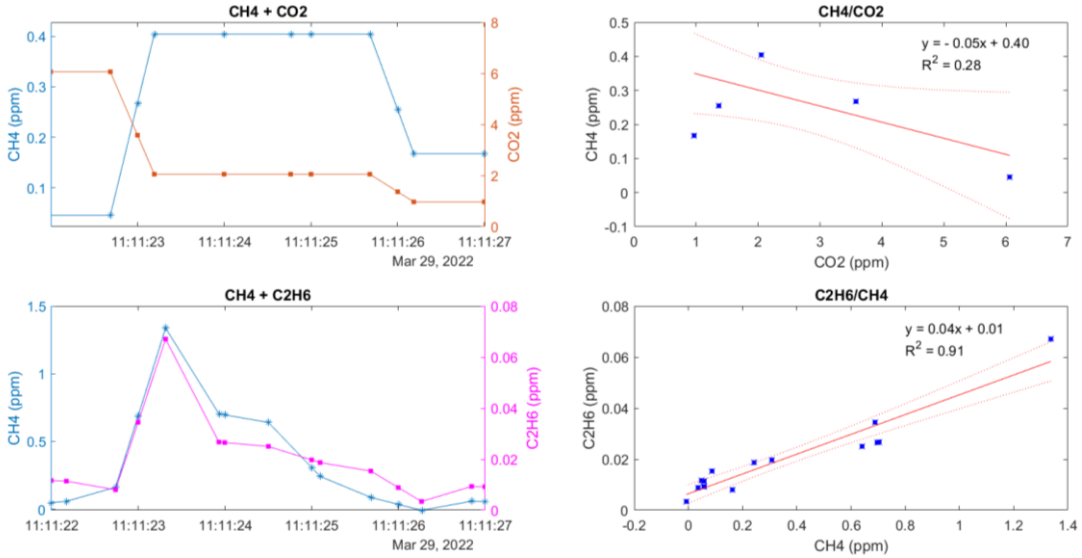

Figure 13: CH_4:CO_2 (above) and C_2H_6:CH_4 (below) correlation graphs from the second transect at location 67 on March 29, 2022. Left: enhancement concentrations over time; right: correlation between compounds, linear regression equation and correlation coefficient.

4. CONCLUSIONS AND FUTURE WORK

The results of this research support those obtained in previous studies. Firstly, it supports all previous studies that have employed this method for mapping cities (Defratyka et al., 2021; Fernandez et al., 2020; Jackson et al., 2014; Luetschwager et al., 2021; Maazallahi et al., 2020; Phillips et al., 2013; von Fischer et al., 2019; Weller et al., 2020) since we also conclude that it is useful and practical for the detection and quantification of leaks from the natural gas distribution network. Moreover, neither CH_4 mobile surveys nor studies focused on emissions from the NG distribution network had been carried out in Amsterdam. Therefore, this project can contribute to current inventories and encourage further surveying efforts in other cities, not only within the country but also internationally.

This study highlights the importance and advantages of adopting a quick and effective method to find leaks since, in most cities, a small proportion of leaks emits the majority of CH_4. The biggest leak that we found accounted for 56% of the total calculated CH_4 emissions. Moreover, this leak was unlikely to be found by the local gas company because it was in an industrial area and is therefore not considered as dangerous as the ones in residential areas, closer to homes (R. van Eekelen, personal communication, June 3, 2022). One of the issues with the current legislation, as was discussed during an interview with one of the policy advisors at the local gas company, is that safety is the only priority, fixing leaks that could potentially be dangerous. Reducing large CH_4 emissions is not a priority. This and the fact that the company is only required to do a survey every five years, could have resulted in very large emissions from just this one leak (63 tons of CH_4 per year).

The method proposed in this study does not guarantee detection of all leaks. However, we were able to find 73% of the leaks on the first drive. That includes elevated CH_4 mixing ratios and C_2H_6:CH_4 correlation. And the probability of detection rises with sampling effort i.e. more transects. This is why even though 29% of LIs were not detected on the first drive, other factors such as height of enhancement peak and plume shape were enough for a revisit. What is clear is that measuring by car is much faster than measuring on foot, which is how gas companies currently look for leaks, and therefore the frequency of surveys could be increased and the big leaks could be detected and fixed quicker. However, mobile surveys are not a substitute and by combining this method with the company's current walking method, it would increase the probability of finding the smaller leaks, which are more difficult to detect.

Regarding the measurements and driving strategy, some changes could be made to optimize the technique, for example, using an algorithm to calculate the most effective way of covering all the streets in a city. This would save time that could be used to do not one but two full drives of the entire study area. Consequently, this would provide more robust information on LIs before performing transects and the number of locations to revisit would be optimal. A total number of 8 transects at each location spread over several hours would be enough for accurate quantification of emissions. Furthermore, mobile measurements on a bike could also be considered because it would be non-polluting and quite useful in some of the busier areas of cities because it is faster than driving. However, smaller equipment is needed for that and, even though the G4302 is portable, it only measures CH_4 and C_2H_6, so this makes new instrumentation necessary, i.e., an instrument that measures CH_4, C_2H_6 and CO_2.

The quantification method used so far is instrument dependent, i.e., specific to the G2301, which is something that can also be improved in future work. Peak area should be used instead of enhancement above background, and a set of controlled release experiments could be carried out to make the equation used for estimating leak emission rates instrument independent. Also, as discussed in the previous section, other factors such as wind, soil conditions and distance between the car and the LIs could be taken into account. Moreover, a different method could be developed so that the emission rates could also be estimated from data from close-up measurements with the G4302 and compared to the results obtained with the other method.

Regarding the criteria for elevated readings, also referred to as enhancements, the C_2H_6 threshold should be increased given that mixing ratios are often elevated but there is not always apparent correlation with CH_4 values. On the contrary, it could be useful to lower the CH_4 detection threshold in the case of small leaks, since it has been mentioned in this study as well as in previous ones (von Fischer et al., 2017; Weller et al., 2018) that the quantification equation tends to be overestimate of the smaller leaks. On the other hand, since the C_2H_6 mode on the G4302 appears to be very useful but faulty at times, some LIs were more difficult to confirm as gas leaks. Therefore, isotopic analysis of specific LIs would help complement and corroborate our findings.

Overall, as future work, more effort should be put into spreading awareness and involving local, regional and national governments in order to bring more attention to the potential of CH_4 emission reductions simply by fixing leaks from the NG distribution network and to exert pressure to change the current legislation. Also, emphasis should be put on the monetary value of using this method in terms of both surveying efforts and reduction of fugitive emissions. The two large leaks that were fixed by the gas company as a result of our study account for 76% of the total calculated emissions. This is equivalent to a cost of approximately 150,000 euros per year for the end user, if the leaks continued for a whole year. According to the CH_4 emissions inventory of Amsterdam, distribution of NG is the cause of 11% of the total yearly emissions. Therefore, tackling these fugitive emissions could have a significant impact and would bring us closer to the Paris Agreement temperature goal and the 30% CH_4 reduction aim by 2030, a global pledge announced at COP26 where more than a hundred countries committed.

In conclusion, the mobile approach is practical, quick and cost-effective. It is most successful for identifying the largest leaks, which contribute disproportionately to total emissions. Further improvements in the quantification method will likely increase accuracy and efficacy for prioritizing leak repair and pipeline management. Lastly, this study has contributed to the reduction of CH_4 emissions in the city of Amsterdam and aims to play a part in the improvement of NG distribution network management as well as to bring more attention to the need for mitigation strategies and partnerships, at both global and city-specific level.

5. REFERENCES

Ars, S., Vogel, F., Arrowsmith, C., Heerah, S., Knuckey, E., Lavoie, J., Lee, C., Pak, N. M., Phillips, J. L., & Wunch, D. (2020). Investigation of the spatial distribution of methane sources in the greater Toronto area using mobile gas monitoring systems. *Environmental Science & Technology*, *54* (24), 15671-15679. https://doi.org/10.1021/acs.est.0c05386

CBS. (2021, February 17). *92 percent homes on natural gas at the beginning of 2019*. https://www.cbs.nl/nl-nl/nieuws/2021/07/92-procent-woningen-op-aardgas-begin-2019

City of Amsterdam. (2020). *Policy: Phasing out natural gas*. https://www.amsterdam.nl/en/policy/sustainability/policy-phasing-out/

Curran, S. J., Wagner, R. M., Graves, R. L., Keller, M., & Green Jr, J. B. (2014). Well-to-wheel analysis of direct and indirect use of natural gas in passenger vehicles. *Energy*, *75*, 194-203. https://doi.org/10.1016/j.energy.2014.07.035

Defratyka, S. M., Paris, J. D., Yver-Kwok, C., Fernandez, J. M., Korben, P., & Bousquet, P. (2021). Mapping urban methane sources in Paris, France. *Environmental Science and Technology*, *55*(13), 8583-8591. https://doi.org/10.1021/acs.est.1c00859

Emission registration. (2022). *Dataset ER series 1990-2019 final plus estimates 2020*. https://www.emissieregistratie.nl/data

ENVI-met GmbH. (2022). ENVI-met (Version 5.0.0) [Computer software]. https://www.envi-met.com/

Fernandez, J. M., Maazallahi, H., France, J. L., Menoud, M., Corbu, M., Ardelean, M., Calcan, A., Townsend-Small, A., van der Veen, C., Fisher, R.E., Lowry, D., Nisbet, E.G. & Röckmann, T. (2022). Street-level methane emissions of Bucharest, Romania and the dominance of urban wastewater. *Atmospheric Environment: X*, *13*, 100153. https://doi.org/10.1016/j.aeaoa.2022.100153

Forman, A. (2014). Caution Ahead: Overdue Investments for New York's Aging Infrastructure. *Center for an Urban Future*. https://nycfuture.org/pdf/Caution-Ahead.pdf

Gallagher, M. E., Down, A., Ackley, R. C., Zhao, K., Phillips, N., & Jackson, R. B. (2015). Natural gas pipeline replacement programs reduce methane leaks and improve consumer safety. *Environmental Science and Technology Letters*, *2* (10), 286-291. https://doi.org/10.1021/acs.estlett.5b00213

Gioli, B., Toscano, P., Lugato, E., Matese, A., Miglietta, F., Zaldei, A., & Vaccari, F. P. (2012). Methane and carbon dioxide fluxes and source partitioning in urban areas: The case study of Florence, Italy. *Environmental Pollution*, *164*, 125-131. https://doi.org/10.1016/j.envpol.2012.01.019

Global Carbon Project. (2020, July 15). *Global Methane Budget*. https://www.globalcarbonproject.org/methanebudget/

Global Methane Initiative. (2011). *Global methane emissions and Mitigation Opportunities*. Retrieved January 14, 2022, from https://www.globalmethane.org/documents/analysis_fs_en.pdf

Helfter, C., Tremper, A. H., Halios, C. H., Kotthaus, S., Bjorkegren, A., Grimmond, C. S. B., Barlow, J. F., & Nemitz, E. (2016). Spatial and temporal variability of urban fluxes of methane, carbon monoxide and carbon dioxide above London, UK. *Atmospheric Chemistry and Physics*, *16* (16), 10543-10557. https://doi.org/10.5194/acp-16-10543-2016

Hendrick, M. F., Ackley, R., Sanaie-Movahed, B., Tang, X., & Phillips, N. G. (2016). Fugitive methane emissions from leak-prone natural gas distribution infrastructure in urban environments. *Environmental Pollution*, 213, 710–716. https://doi.org/10.1016/j.envpol.2016.01.094

Hopkins, F. M., Ehleringer, J. R., Bush, S. E., Duren, R. M., Miller, C. E., Lai, C.-T., Hsu, Y.-K., Carranza, V., & Randerson. J. T. (2016). Mitigation of methane emissions in cities: How new measurements and partnerships can contribute to emissions reduction strategies. *Earth's Future*, *4*, 408–425. https://doi.org/10.1002/2016EF000381

IEA. (2021). *Methane Emissions from Oil and Gas*. IEA, Paris. https://www.iea.org/reports/methane-emissions-from-oil-and-gas

IPCC, 2021: *Climate Change 2021: The Physical Science Basis. Contribution of Working Group I to the Sixth Assessment Report of the Intergovernmental Panel on Climate Change* [Masson-Delmotte, V., P. Zhai, A. Pirani, S.L. Connors, C. Péan, S. Berger, N. Caud, Y. Chen, L. Goldfarb, M.I. Gomis, M. Huang, K. Leitzell, E. Lonnoy, J.B.R. Matthews, T.K. Maycock, T. Waterfield, O. Yelekçi, R. Yu, and B. Zhou (eds.)]. Cambridge University Press, Cambridge, United Kingdom and New York, NY, USA, 2391 pp. https://doi.org/10.1017/9781009157896

IPCC, 2022: *Climate Change 2022: Impacts, Adaptation and Vulnerability. Contribution of Working Group II to the Sixth Assessment Report of the Intergovernmental Panel on Climate Change* [H.-O. Pörtner, D.C. Roberts, M. Tignor, E.S. Poloczanska, K. Mintenbeck, A. Alegría, M. Craig, S. Langsdorf, S. Löschke, V. Möller, A. Okem, B. Rama (eds.)]. Cambridge University Press. Cambridge University Press, Cambridge, UK and New York, NY, USA, 3056 pp., https://doi.org/10.1017/9781009325844

Jackson, R. B., Down, A., Phillips, N. G., Ackley, R. C., Cook, C. W., Plata, D. L., & Zhao, K. (2014). Natural gas pipeline leaks across Washington, DC. *Environmental science and technology*, *48* (3), 2051-2058. https://doi.org/10.1021/es404474x

Liander. (2022). *Gas replacement data. Gray cast iron and asbestos cement pipes.* https://www.arcgis.com/home/item.html?id=06f05645167b42f9b24a42fc90035c9f

Lowry, D., Holmes, C. W., Rata, N. D., & Nisbet, E. G. (2001). London methane emissions: Use of diurnal changes in concentration and $\delta^{13}C$ to identify urban sources and verify inventories. J. *Geophys. Res.*, 106 (D7), 7427-7448. https://doi.org/10.1029/2000JD900601

Luetschwager, E., von Fischer, J. C., & Weller, Z. D. (2021). Characterizing detection probabilities of advanced mobile leak surveys: Implications for sampling effort and leak size estimation in natural gas distribution systems. *Elem Sci Anth*, *9* (1), 00143. https://doi.org/10.1525/elementa.2020.00143

Maazallahi, H., Delre, A., Scheutz, C., Fredenslund, A. M., Schwietzke, S., Denier van der Gon, H., & Röckmann, T. (2022). Intercomparison of detection and quantification methods for methane emissions from the natural gas distribution network in Hamburg, Germany. *Atmospheric Measurement Techniques Discussions*, 1-29. https://doi.org/10.5194/amt-2022-134

Maazallahi, H., Fernandez, J. M., Menoud, M., Zavala-Araiza, D., Weller, Z. D., Schwietzke, S., von Fischer, J. C., van der Gon, H. D., & Röckmann, T. (2020). Methane mapping, emission

quantification, and attribution in two European cities: Utrecht (NL) and Hamburg (DE). *Atmospheric Chemistry and Physics*, *20* (23), 14717-14740. https://doi.org/10.5194/acp-20-14717-2020

Marcotullio, P. J., Sarzynski, A., Albrecht, J., Schulz, N., & Garcia, J. (2013). The geography of global urban greenhouse gas emissions: An exploratory analysis. *Climatic Change*, *121*(4), 621-634. https://doi.org/10.1007/s10584-013-0977-z

McKain, K., Down, A., Raciti, S. M., Budney, J., Hutyra, L. R., Floerchinger, C., Herndon, S. C., Nehrkorn, T., Zahniser, M. S., Jackson, R. B., Phillips, N., & Wofsy, S. C. (2015). Methane emissions from natural gas infrastructure and use in the urban region of Boston, Massachusetts. *Proceedings of the National Academy of Sciences*, *112* (7), 1941-1946. https://doi.org/10.1073/pnas.1416261112

Myhre, G., Shindell, D., Bréon, F. M., Collins, W., Fuglestvedt, J., Huang, J., Koch, D., Lamarque, J. F., Lee, D., Mendoza, B., Nakajima, T., Robock, A., Stephens, G., Takemura, T., & Zhang, H. (2013). *Anthropogenic and Natural Radiative Forcing.* In *Climate Change 2013: The Physical Science Basis*. Cambridge University Press, Cambridge, United Kingdom and New York, NY, USA.

Nam, E. K., Jensen, T. E., & Wallington, T. J. (2004). Methane emissions from vehicles. *Environmental science & technology*, *38* (7), 2005-2010. https://doi.org/10.1021/es034837g

NOAA. (2022, June 5). *Trends in atmospheric methane*. NOAA Global Monitoring Laboratory. https://gml.noaa.gov/ccgg/trends_ch4/

Open Street Map Data Extracts. (2022). Open Street Map.
http://download.geofabrik.de/europe/netherlands/noord-holland.html

Phillips, N. G., Ackley, R., Crosson, E. R., Down, A., Hutyra, L. R., Brondfield, M., Karr, J. D., Zhao, K., and Jackson, R. B. (2013). Mapping urban pipeline leaks: Methane leaks across Boston. *Environmental Pollution, 173*, 1–4. https://doi.org/10.1016/j.envpol.2012.11.003

Picarro. (2017). G4302 Gas Scouter datasheet. https://www.sanyo-si.com/wp-content/uploads/Datasheet-G4302-GasScouter-for-CH4-and-C2H6-in-Air.pdf

Picarro. (2021). G2301 Analyzer datasheet.
https://www.picarro.com/support/library/documents/g2301_analyzer_datasheet

Plant, G., Kort, E. A., Floerchinger, C., Gvakharia, A., Vimont, I., & Sweeney, C. (2019). Large fugitive methane emissions from urban centers along the U.S. East Coast. *Geophysical Research Letters*, 46, 8500–8507. https://doi.org/10.1029/2019GL082635

Prather, M. J., Holmes, C. D., and Hsu, J. (2012), Reactive greenhouse gas scenarios: Systematic exploration of uncertainties and the role of atmospheric chemistry, *Geophys. Res. Lett.*, 39, L09803. https://doi.org/10.1029/2012GL051440

Sargent, M. R., Floerchinger, C., McKain, K., Budney, J., Gottlieb, E. W., Hutyra, L. R., Rudek, J., & Wofsy, S. C. (2021). Majority of US urban natural gas emissions unaccounted for in inventories. *Proceedings of the National Academy of Sciences*, *118*(44). https://doi.org/10.1073/pnas.2105804118

Saunois, M., Stavert, A. R., Poulter, B., Bousquet, P., Canadell, J. G., Jackson, R. B., ... & Zhuang, Q. (2020). The global methane budget 2000–2017. *Earth system science data*, *12*(3), 1561-1623. https://doi.org/10.5194/essd-12-1561-2020

Van Amstel, A. (2012). Methane. A review. *Journal of Integrative Environmental Sciences*, 9:sup1, 5-30. https://doi.org/10.1080/1943815X.2012.694892

Veenhuysen, D., & Hofschreuder, P. (1995). Methane emission of the Amsterdam urban area. *Studies in Environmental Science*, 65, 603-606. https://doi.org/10.1016/S0166-1116(06)80252-9

von Fischer, J. C., Cooley, D., Chamberlain, S., Gaylord, A., Griebenow, C. J., Hamburg, S. P., Salo, J., Schumacher, R., Theobald, D., & Ham, J. (2017). Rapid, vehicle-based identification of location and magnitude of urban natural gas pipeline leaks. *Environmental Science & Technology*, *51* (7), 4091-4099. https://doi.org/10.1021/acs.est.6b06095

Weller, Z. D., Hamburg, S. P., & von Fischer, J. C. (2020). A national estimate of methane leakage from pipeline mains in natural gas local distribution systems. *Environmental science & technology*, *54* (14), 8958-8967. https://doi.org/10.1021/acs.est.0c00437

Weller, Z. D., Roscioli, J. R., Daube, W. C., Lamb, B. K., Ferrara, T. W., Brewer, P. E., & von Fischer, J. C. (2018). Vehicle-based methane surveys for finding natural gas leaks and estimating their size: Validation and uncertainty. *Environmental science & technology*, *52* (20), 11922-11930. https://doi.org/10.1021/acs.est.8b03135

Weller, Z. D., Yang, D. K., & von Fischer, J. C. (2019). An open-source algorithm to detect natural gas leaks from mobile methane survey data. *PLoS One*, *14* (2), e0212287. https://doi.org/10.1371/journal.pone.0212287

Wever, D., Dröge, P. W. H. G., Geilenkirchen, G. P., van Huijstee, J., t Hoen, M., Honig, E., te Molder, R. A. B., Smeets, W. L. M., Zanten, M. C., & van der Zee, T. (2022). Informative Inventory Report 2022. Emissions of transboundary air pollutants in the Netherlands 1990–2020. https://rivm.openrepository.com/handle/10029/625729

SI. SUPPLEMENTARY INFORMATION

SI.1. Instrumentation

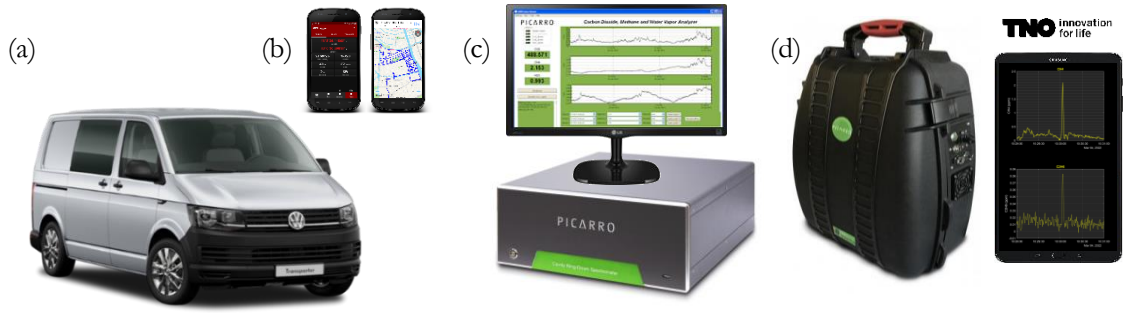

Figure 14: Measurement setup. (a) Volkswagen Transporter (https://www.nicepng.com/); (b) GPS tracker; (c) G2301analyzer (Picarro, 2021); (d) G4302 analyzer (Picarro, 2017).

Figure 15: Pictures of the measurement setup.

SI.2. Weather dependency

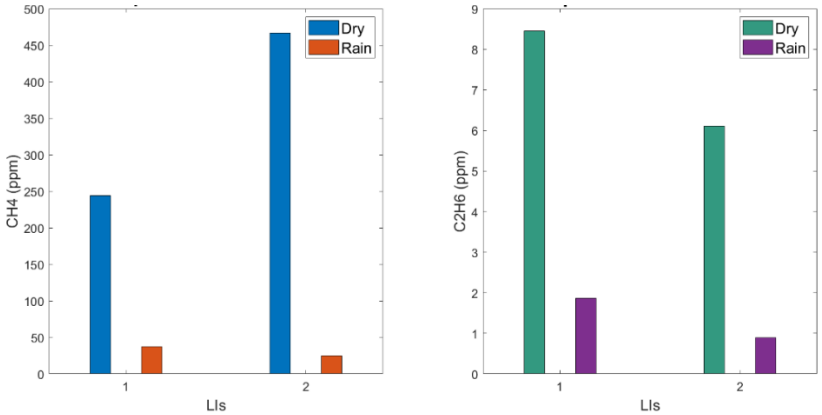

Figure 16: Impact of rain on the G4302 analyzer measurements for both CH_4 and C_2H_6 directly at the source.

SI.3. Measurement surveys log

Table 7: Information about all mobile measurements.

Date	Time		Focus Area	Time correction (seconds)	
	Start (UTC)	End (UTC)		G2301	G4302
4-Nov-21	10:00	15:00	Watergraafsmeer	45	-62
15-Nov-21	9:00	15:00	Watergraafsmeer	55	-80
2-Dec-21	11:00	16:00	Watergraafsmeer	68	-4
7-Feb-22	9:30	16:15	Watergraafsmeer	-15	-4
8-Feb-22	8:30	16:00	De Pijp	-16	-5.5
9-Feb-22	8:00	15:30	De Pijp	-15	-5.5
10-Feb-22	11:30	16:20	Port of Amsterdam	-15	-8
11-Feb-22	8:30	16:00	De Pijp	-14	-8
28-Feb-22	10:00	16:00	Port of Amsterdam	-9	-2
2-Mar-22	9:00	17:00	Watergraafsmeer	-7	-4
3-Mar-22	9:00	15:30	De Pijp, Rivierenbuurt	-7	-4
4-Mar-22	9:00	16:45	De Pijp, Oud-Oost	-6	-5
14-Mar-22	9:00	16:30	Oosterparkbuurt, Plantage	-46	-63
15-Mar-22	8:00	15:00	Rivierenbuurt, De Pijp, Watergraafsmeer	-44	-63
17-Mar-22	8:00	15:30	Oosterparkbuurt	-40	-60
28-Mar-22	8:00	15:00	Weesperbuurt, Plantage	-37	-3.5
29-Mar-22	8:00	15:00	Weesperbuurt, Oosterparkbuurt, De Pijp	-39	-3
30-Mar-22	9:00	16:00	Weesperbuurt, Oosterparkbuurt, Oud-Zuid	-37	-5
31-Mar-22	7:30	9:30	De Pijp, Oosterparkbuurt	-36	-7
14-Apr-22	7:30	16:30	Oud-Zuid	-32	-29.5
15-Apr-22	8:30	18:00	Weesperbuurt, Zeeburg, Dapperbuurt	-28	-30.5
16-Apr-22	8:30	14:00	Oud-Zuid, Zeeburg	-28	-32
19-Apr-22	9:30	12:30	Oud-Zuid, Weesperbuurt, Dapperbuurt	-28.5	-34

SI.4. High confidence LIs

Table 8: Information of all high confidence LIs (33), where C_2H_6:CH_4 correlation was observed at least twice. Detection probabilities are only calculated for LIs with a minimum of 8 drives and at least one drive above the 10% threshold.

							Detection Probability			CH_4:C_2H_6 Correlation		
LI num	Lat	Lon	Highest enh (ppm)	Drives	Drives > 10%	Rate L min^{-1}	G2301 CH_4	G4302 CH_4	G4302 C_2H_6	Prob %	Slope	R^2
1	52.3558	4.9396	1.96	32	8	1.04	100%	100%	100%	62%	0.03	0.92
6	52.3531	4.9283	2.61	29	19	1.70	100%	100%	95%	95%	0.04	0.96
9	52.3415	4.9449	0.69	1	1	2.13						
11	52.3624	4.9395	0.17	10	0	-						
32	52.3475	4.9405	0.35	10	3	0.73	30%	40%	70%	10%	0.07	0.92
45	52.3532	4.8945	4.92	12	11	3.13	92%	83%	100%	75%	0.05	0.95
49	52.3567	4.9048	0.54	12	5	1.14	42%	33%	100%	17%	0.03	0.73
50	52.4058	4.8563	1.87	5	3	2.11						
51	52.3995	4.7880	2.66	10	10	3.33	100%	100%	100%	100%	0.03	0.79
55	52.3533	4.9034	1.85	23	22	2.12	87%	87%	91%	74%	0.03	0.90
60	52.4107	4.8005	45.51	16	16	166.10	100%	100%	100%	100%	0.04	0.94
61	52.4013	4.7992	24.98	23	20	7.04	100%	100%	100%	100%	0.04	0.94
62	52.3490	4.883	4.62	28	16	2.65	16%	28%	66%	22%	0.04	0.80
63	52.3478	4.8607	0.74	21	12	0.99	65%	83%	96%	62%	0.04	0.89

67	52.3515	4.8861	2.36	23	19	1.71	95%	95%	100%	61%	0.04	0.88
70	52.3510	4.9354	0.12	8	0	-						
71	52.3661	4.9344	0.61	3	2	1.24						
76	52.3447	4.8850	42.37	22	22	58.54	57%	64%	78%	46%	0.04	0.89
91	52.3577	4.9107	7.47	37	37	4.84	57%	62%	81%	19%	0.02	0.75
93	52.3588	4.9129	1.12	23	16	1.22	83%	87%	96%	65%	0.04	0.88
94	52.3602	4.9096	1.17	3	2	2.31						
95	52.3566	4.9117	1.84	17	10	2.64	100%	100%	100%	92%	0.03	0.90
97	52.3621	4.9117	1.85	25	16	1.04	70%	87%	78%	39%	0.03	0.85
98	52.3641	4.9108	0.89	19	6	0.99	59%	65%	76%	70%	0.04	0.87
100	52.3625	4.9198	9.09	27	24	3.66	58%	73%	69%	42%	0.03	0.86
101	52.3552	4.9285	0.55	20	14	0.83	31%	37%	79%	21%	0.04	0.82
111	52.3603	4.9054	0.57	3	1	1.70						
112	52.3636	4.9062	1.06	5	2	1.35						
114	52.3626	4.9072	2.2	24	24	2.83	89%	89%	100%	81%	0.03	0.88
115	52.3658	4.9052	4.11	13	13	7.80	70%	70%	75%	50%	0.04	0.81
117	52.4107	4.8287	5.82	9	9	8.57	100%	100%	96%	75%	0.03	0.85
134	52.3537	4.8816	0.783	13	5	1.12	39%	62%	92%	46%	0.04	0.79
136	52.3634	4.8532	0.36	2	2	0.76						

SI.5. Low confidence LIs

Table 9: Information of all low confidence LIs (11), where C_2H_6:CH_4 correlation was observed only once.

LI num	Lat	Lon	Highest enh (ppm)	Drives	Drives > 10%	Rate (L min^{-1})
18	52.3438	4.9263	0.09	7	0	
82	52.3514	4.9155	2.35	1	1	9.5506
84	52.3537	4.9193	0.32	3	2	0.4884
88	52.3575	4.927	0.15	3	0	
99	52.367	4.9092	0.59	3	1	1.771
103	52.3328	4.9235	3.16	1	1	13.682
121	52.3474	4.8623	0.3	12	3	0.6984
142	52.3598	4.9395	0.82	1	1	2.6453
145	52.3613	4.9079	0.14	2	0	
151	52.3573	4.8863	0.26	2	1	0.6413
154	52.3642	4.8473	0.36	1	1	0.9596

SI.6. Pictures of leak locations

Figure 17: Firefighters at leak 60 seizing the area.

Figure 18: Leak 76 after reparations by local gas company.

Figure 19: Outlet locations of LIs 114, 115, 100, 63, 98 and 93.

SI.7. G2301 & G4302 correlation

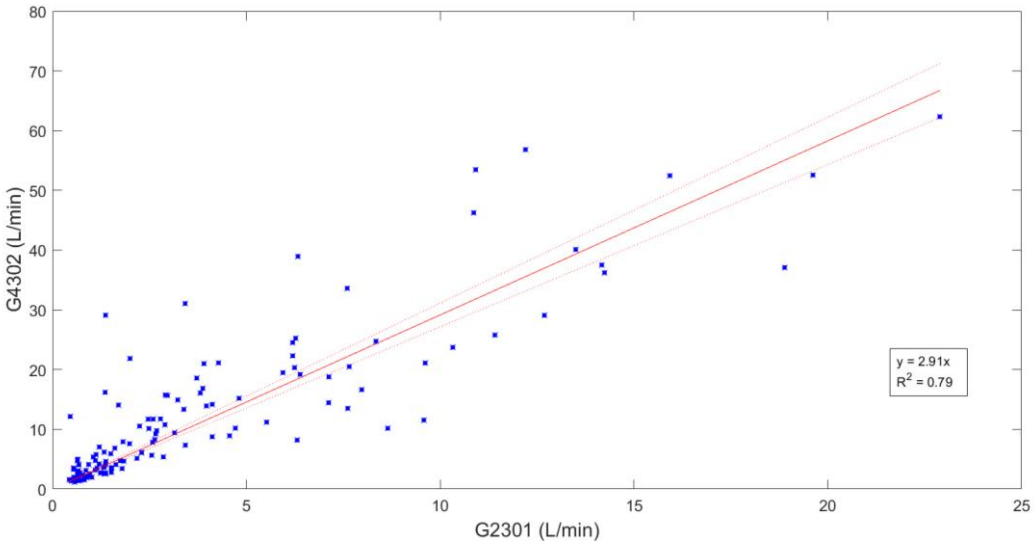

Figure 20: Correlation plot of emission rates for comparison of G2301 and G4302.

SI.8. Measurements at location 67

Table 10: Information from all drives at location 67 on February 11 and March 29. The local gas company classified this LI as swamp gas after it was reported by us.

				G2301 (ppm)		G4302 (ppm)		Correlation R^2	
	Lap	Lat	Lon	CH_4 enh	CO_2 enh	CH_4 enh	C_2H_6 enh	CH_4:CO_2	C_2H_6:CH_4
February 11	1	52.3516	4.8861	0.19	56.80	0.54	0.02	-	0.71
	2	52.3530	4.8931	0.33	38.62	0.71	0.30	-	-
	3	52.3516	4.8861	1.09	66.40	4.05	0.21	-	0.93
	4	52.3515	4.8861	0.55	4.19	1.79	0.08	-	0.96
	5	52.3514	4.8860	0.46	10.71	1.06	0.05	0.80	0.82
	6	52.3516	4.8861	0.43	2.85	1.21	0.06	-	0.93
	7	52.3515	4.8861	0.48	8.04	1.19	0.05	-	0.91
	8	52.3513	4.8861	0.27	41.58	0.49	0.03	-	0.72
	9	52.3516	4.8861	0.81	4.69	2.78	0.11	0.99	0.97
	10	52.3509	4.8869	0.17	0.21	0.27	0.02	-	-
March 29	1	52.3515	4.8860	0.30	113.01	0.74	0.02	0.99	-
	2	52.3516	4.8861	0.40	2.05	1.34	0.07	-	0.90
	3	52.3516	4.8862	0.56	8.94	1.18	0.04	-	-
	4	52.3517	4.8862	0.83	17.41	2.29	0.05	-	0.76
	5	52.3518	4.8862	0.20	8.45	0.52	0.02	0.99	-
	6	52.3517	4.8862	1.22	15.56	4.50	0.18	-	0.98
	7	52.3516	4.8860	0.95	0.71	2.32	0.07	-	0.79
	8	52.3515	4.8861	0.07	14.28	0.13	0.01	0.83	-
	9	52.3514	4.8861	0.60	38.28	1.02	0.03	-	-

Table 11: Close-up measurement at location 67 with the G4302 analyzer on March 2.

G4302 (ppm)		Correlation R^2	
CH_4 enh	C_2H_6 enh	CH_4:CO_2	C_2H_6:CH_4
1294	54.30	-	0.97

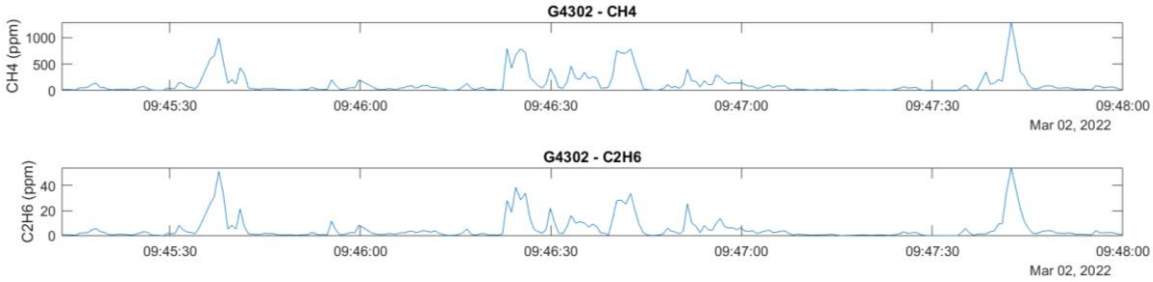

Figure 21: CH_4 and C_2H_6 enhancements from close-up measurement at location 67 with the G4302 analyzer on March 2.

SI.9. Temporal variability

Table 12: Information of daily and total emission rates at all the quantified high confidence LIs.

	Day 1		Day 2		Day 3		Day 4		Day 5		Total
Leak num	**Num drives**	**Rate L min^{-1}**	**Num drives**	**Rate L min^{-1}**	**Num drives**	**Rate L min^{-1}**	**Num drives**	**Rate L min^{-1}**	**Num drives**	**Rate L min^{-1}**	**Rate L min^{-1}**
91	6	3.18	13	5.10	2	5.10	13	3.93	3	21.19	4.84
55	9	1.46	2	3.36	1	1.18	10	2.87			2.12
100	2	14.02	9	2.48	10	4.16	3	3.13			3.74
6	1	1.47	9	1.82	9	1.61					1.70
61	10	5.76	3	91.91	7	3.11					7.04
67	8	1.45	3	3.24	8	1.60					1.71
93	1	0.61	9	1.67	6	0.85					1.22
97	9	1.40	6	0.72	1	0.68					1.04
114	12	4.51	10	1.86	2	1.38					2.83
63	2	0.52	4	1.79	6	0.82					0.99
95	2	5.60	1	2.35	7	2.17					2.64
101	1	0.93	11	0.81	2	0.87					0.83
1	2	2.05	3	0.83	3	0.82					1.04
49	1	1.46	4	1.07							1.14
32	1	0.47	2	0.91							0.73
60	6	162.72	10	168.16							166.10
76	12	32.21	10	119.91							58.54
62	12	3.95	4	0.80							2.65
115	3	5.55	10	8.64							7.80
98	6	0.99									0.99
45	11	3.13									3.13
51	10	3.33									3.33
117	9	8.57									8.57
134	5	1.12									1.12

Table 13: Information of range of enhancements from individual transects and range relative to leak size at all the quantified high confidence LIs.

Leak num	Highest enh (ppm)	Lowest enh (ppm)	Range (ppm)	Rate (L min^{-1})	Range/Rate
1	1.96	0.23	1.73	1.04	1.67
6	2.61	0.2581	2.35	1.70	1.39
55	1.85	0.24	1.61	2.12	0.76
60	45.51	4.63	40.88	166.10	0.25
61	24.98	0.22	24.76	7.04	3.52
62	4.62	2.22	2.40	2.65	0.91
63	0.74	0.20	0.54	0.99	0.55
67	2.36	0.20	2.16	1.71	1.26
76	42.37	0.25	42.12	58.54	0.72
91	7.47	0.23	7.24	4.84	1.50
93	1.12	0.22	0.90	1.22	0.74
95	1.84	0.33	1.51	2.64	0.57
97	1.85	0.20	1.65	1.04	1.59
98	0.89	0.23	0.66	0.99	0.67
100	9.09	0.24	8.85	3.66	2.42
101	0.55	0.22	0.33	0.83	0.39
114	2.2	0.30	1.90	2.83	0.67
115	4.11	0.88	3.23	7.80	0.41
117	5.82	0.62	5.20	8.57	0.61
45	4.92	0.21	4.71	3.13	1.51
51	2.66	0.59	2.07	3.33	0.62

SI.10. Detection probability

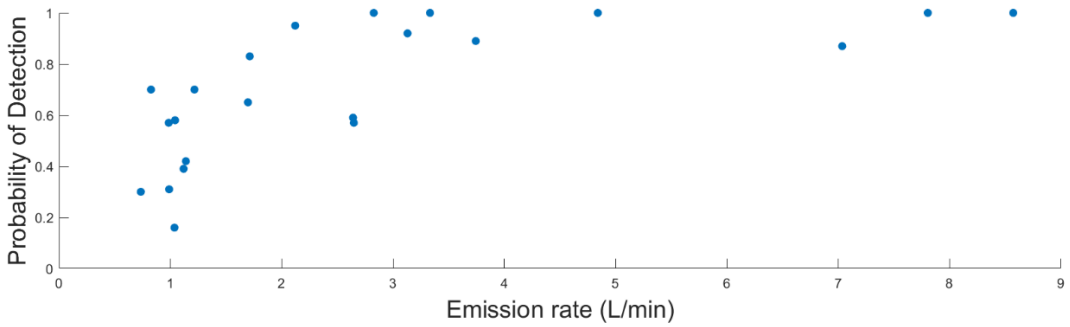

Figure 22: Probability of CH_4 detection with the G2301 analyzer as a function of emission rate. The two high-rate leaks are excluded for better visualization since both their detection probabilities are 100%.

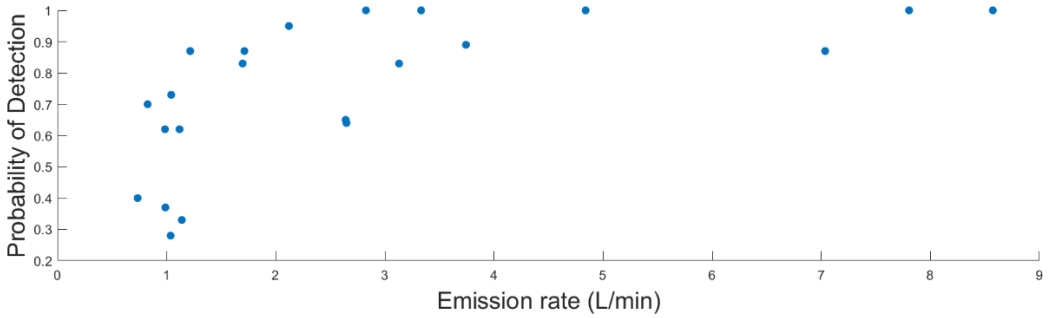

Figure 23: Probability of CH_4 detection with the G4302 analyzer as a function of emission rate. The two high-rate leaks are excluded for better visualization since both their detection probabilities are 100%.

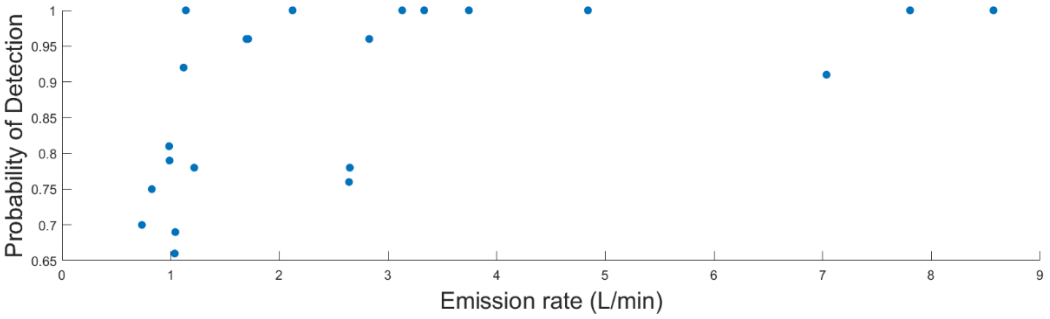

Figure 24: Probability of C_2H_6 detection with the G2301 analyzer as a function of emission rate. The two high-rate leaks are excluded for better visualization since their detection probabilities are 100% and 95%.